Mon. Not. R. Astron. Soc. **335,** 853–863 (2002)

Brown dwarfs in the Pleiades: spatial distribution and mass function

R. F. Jameson,[1⋆] P. D. Dobbie,[1] S. T. Hodgkin[2] and D. J. Pinfield[3]

[1]*Astronomy Group, Department of Physics and Astronomy, University of Leicester, University Road, Leicester LE1 7RH*
[2]*Institute of Astronomy, Madingley Road, Cambridge CB3 0HA*
[3]*Astrophysics Research Institute, Liverpool John Moores University, Birkenhead, CH41 1LD*

Accepted 2002 May 8. Received 2002 May 7; in original form 2002 April 10

ABSTRACT

Using new infrared data we have reassessed the membership status of candidate low-mass Pleiads unearthed by the International Telescope Project *I Z* survey. Those with *I–K* colours consistent with membership of the Pleiades have been compiled with candidate brown dwarfs identified by three other large, deep far-red CCD surveys of the cluster to yield the biggest magnitude-limited sample of substellar members to date. We fit King profiles to their spatial distribution to determine the Pleiades brown dwarf core radius to be $r_c = 2.22^{+1.36}_{-0.67}$ degrees (or $5.0^{+3.0}_{-1.5}$ pc). This is consistent with a continuation of the $r_c \propto m^{-0.5}$ relationship found previously for the higher-mass stellar members and suggests that the brown dwarf members are also dynamically relaxed. Using our spatial model we derive the Pleiades mass function in the substellar regime and are able to place stringent limits on its shape. We find that it is well represented by a power law with index $\alpha = 0.41 \pm 0.08$ ($0.035\ M_\odot \lesssim M \lesssim 0.3\ M_\odot$). This result is largely insensitive to our choice of evolutionary model and uncertainties in the cluster age and distance. It is only marginally sensitive to the brown dwarf binary fraction. By assuming that the cluster mass function continues to rise down to the deuterium-burning limit, we estimate that the total brown dwarf mass of the Pleiades is $13^{+4}_{-3}\ M_\odot$. This only represents ∼2 per cent of the total cluster mass. Given that the present-day cluster mass function should be a good representation of the initial mass function, we conclude that brown dwarfs do not contribute significantly to disc dark matter.

Key words: stars: low-mass, brown dwarfs – stars: luminosity function, mass function – open clusters and associations: individual: Pleiades – infrared: stars.

1 INTRODUCTION

It has long been recognized that the Pleiades open (galactic) cluster is a very suitable hunting ground for brown dwarfs (BDs) (e.g. Jameson & Skillen 1989; Stauffer et al. 1989). The cluster is nearby, but not so close as to cover a very large area of sky. It is also young, so any BDs have not had much time to cool and are therefore comparatively bright. Furthermore one might hope that the present-day cluster mass function would provide a reasonable measure of the initial mass function, which contains information on the process of star formation (e.g. Adams & Fatuzzo 1996; Elmegreen 2000). One of the original scientific motivations for searching for BDs was to see if they might make a significant contribution to disc dark matter, which is inferred from various 'stellar tracer' populations (e.g. Bahcall, Flynn & Gould 1992).

Estimation of both the luminosity and mass functions for the entire Pleiades cluster requires a knowledge of how the stars and BDs are distributed. It is well known that the lower-mass stars in an open cluster are more widely spread than the high-mass stars (e.g. Spitzer & Mathieu 1980). Thus a survey of the central regions of the Pleiades will not be representative of the cluster as a whole. The cluster spatial distribution can be modelled by a King profile (King 1962). An important parameter of this distribution is the core radius, the radius at which the surface density of members falls to half its central value. The core radius is known to vary with stellar mass (Pinfield, Jameson & Hodgkin 1998). Thus to obtain the mass function of the whole cluster we need to determine the core radii for both the stars and the BDs.

In this paper we bring together data from the four largest optical surveys for Pleiades BDs. We determine the core radius of the Pleiades BDs and place stringent constraints on the cluster luminosity and mass functions in the substellar regime. In the next section we briefly review, in turn, the four optical surveys. We discuss the photometric systems used by each and develop prescriptions to transform all *I* photometry onto the I_C system. In Section 3 we present our follow-up *K*-band photometry for candidate Pleiads from the ITP (Zapatero-Osorio et al. 1999) and the CFHT (Bouvier et al. 1998)

⋆E-mail: pdd@star.le.ac.uk

surveys. We construct an I, I–K colour–magnitude diagram (CMD) and from this draw a refined list of probable substellar cluster members. In Section 4 we examine the spatial distribution of cluster BDs and attempt to measure their core radius. Finally we use our new estimate of core radius to derive the cluster luminosity and mass functions presented in Section 5.

2 THE OPTICAL CCD SURVEYS

To construct luminosity and mass functions for the Pleiades we consider the four largest area optical surveys to date. These are, in no particular order, the International Telescope Project (ITP) survey (Zapatero-Osorio et al. 1997c, 1999), the Canada France Hawaii Telescope (CFHT) survey (Bouvier et al. 1998), the Burrell Schmidt (BPL) survey (Pinfield et al. 2000) and the INT Wide Field Camera (IWFC) survey (Dobbie et al. 2002a). We note that Adams et al. (2001) have surveyed the entire cluster for stellar members down to $\sim$0.1 $M_\odot$ using 2MASS near-infrared photometry and proper motions derived from POSS plates digitized by the USNO PMM program.

2.1 The ITP survey

A deep IZ survey covering $\sim$1 square degree in the central region of the Pleiades cluster is presented by Zapatero-Osorio et al. (1999). In their table 2 they list a total of 47 candidates with I magnitudes in the range 17.3–22.3, which were selected on the the basis of their position in the I, I–Z CMD. The survey is quoted as being complete up to $I_C \sim 21$, $Z \sim 20.5$. One of the faintest of these ITP sources is, to date, the coolest candidate Pleiad for which an optical spectrum has been obtained. The early-L type Roque 25 is discussed in detail by Martín et al. (1998). Optical spectroscopy and infrared photometry for several other ITP sources has been presented by Zapatero-Osorio, Rebolo & Martín (1997a) and Martín et al. (2000).

2.2 The CFHT survey

Bouvier et al. (1998) report the identification of 26 candidate cluster members in a 2.5-square-degrees survey of the Pleiades, complete up to $R \sim 23$ and $I_C \sim 22$ (though the effective survey limit is $I_C \sim 19.5$ for the Pleiades sequence due to the saturation of the R–I colour). They proposed that 17 were substellar. However, more-recently-published infrared data indicate that CFHT-PL-19, CFHT-PL-20 and CFHT-PL-22 are not members of the Pleiades (Martín et al. 2000). An optical spectrum of CFHT-PL-26 and the proper motions of CFHT-PL-14 and CFHT-PL-18 suggest that they too are most probably not cluster members (Martín et al. 2000; Moraux, Bouvier & Stauffer 2001). Hence of the original 17 candidate substellar Pleiads there remain 9 which are not common to the ITP survey.

2.3 The Burrell Schmidt survey

A 6-square-degree IZ survey of the Pleiades undertaken with the Kitt Peak Burrell Schmidt telescope is presented by Pinfield et al. (2000). The survey is quoted as being complete up to $I_C \sim 19.5$, though the large (2-arcsec) pixel scale means that BD candidates close to brighter stars could not be detected owing to blending (e.g. PIZ 1, Cossburn et al. 1997). A total of 30 likely BD candidates was initially proposed on the basis of follow-up K-band photometry and, for the brighter candidates, Schmidt plate proper motions. However, BPL 283 (CFHT-PL-18) does not show the expected litium absorption (Martín et al. 2000) and recently-acquired JHK data (Pinfield et al. 2002, in preparation) indicate that BPL132 (Roque 11), BPL168 and BPL249 are non-members. Here we assume that the remaining 26 of the initial 30 candidates identified by Pinfield et al. (2000) are members of the cluster. Of these, 10 are not duplicated in the ITP and CFHT surveys.

2.4 The INT Wide Field Camera survey

The fourth data set is drawn from a recently-published survey undertaken with the INT telescope and Wide Field Camera (WFC) as part of the Wide Field Survey project (McMahon et al. 2001). Dobbie et al. (2002a) have surveyed an area of 1.1 square degrees of the Pleiades in the I_H and Z_{RGO} bands down to a 90 per cent completeness limit of $I_H \sim 21.8$. A list of 23 likely low-mass members is proposed on the basis of additional follow-up K-band photometry, 15 of which are previously unpublished. The faintest candidate identified by Dobbie et al. (2002a), INT-PL-IZ-69, has a mass of $M \sim 0.03$ $M_\odot$ and may be the coolest Pleiad published to date.

2.5 *I*-band CCD photometry

One of the principle problems when intercomparing CCD surveys is the variety of filter systems in use with different telescopes. Although most observers transform photometry onto a standard system (e.g. I_C), this is fraught with difficulty for very-red stars because of the notable lack of extremely-red standard stars. This is especially true for the R and I passbands where glass and interference CCD filters deviate significantly from the response of the filter–detector combination employed by Landolt.

The I photometry in Zapatero-Osorio et al. (1999) lies on the Harris system – that is to say Harris filters (R_H, I_H) were used with Landolt standards. R_H is a very good match to R_C, but the I_H response is quite different from I_C. For observations calibrated by standards that are not particularly red (as was the case for the ITP survey), there is little difference between the two systems, with the net result that the I-band data to all intents and purposes lie on the Harris system. The I photometry in Dobbie et al. (2002a) was similarly obtained using the Harris I filter of the WFC. However, no attempt was made by those authors to transform the instrumental magnitudes onto the standard I_C system and hence these too lie on the Harris system. Using observed and synthetic photometry drawn from Cossburn et al. (1998), Dobbie et al. (2002b) and the 2MASS Second Incremental Point Source Catalogue (SIPSC) (e.g. Skrutskie et al. 1995), we have derived the equation $I_C - I_H = 0.172(I_H - K) - 0.204$ ($2.3 \leqslant I_H - K \leqslant 5.0$) to transform these magnitudes onto the I_C system. Not surprisingly, Bouvier et al. (1998) and Festin (1998), both of whom made a specific effort to observe a number of very-red standards to ensure that their photometry was reliably transformed onto the Cousins system, have noticed discrepancies between the photometry of Zapatero-Osorio et al. (1999) and their own. We believe these discrepancies are fully explained by the difference in the filter systems. For example, for Teide 1, after applying the transformation, we find $I_C = 19.22$, within a few per cent of Festin, who measures $I_C = 19.26$. For the Roque candidates, the new values are included in Table 1 in preference to the original photometry presented in Zapatero-Osorio et al. (1999). For completeness, we have also listed I_C photometry from the literature where available.

The BPL survey was measured using the Kitt Peak I interference filter. To investigate the relationship between KPNO $I(I_{KP})$ and Cousins I, we have compared synthetic I_{KP} and I_C magnitudes generated using the flux-calibrated spectra of the sample of field

Table 1. Columns 1 and 2 give the outer and average radii for each annulus. Column 3 gives the surveyed area of each annulus. Column 4 gives the number of BDs from our magnitude-limited sample in each annulus. Columns 5, 6 and 7 give the surface density, the annulus area and the inferred magnitude-limited total of BDs in each annulus. The quoted uncertainties stem from counting statistics.

Radius of annulus (°)	r°	Area surveyed (sq. °)	Number of BDs	Surface density (per sq. °)	Area of annulus (sq. °)	Cumulative total
1.0	0.71	1.760	11	6.25 ± 1.88	3.142	19.64 ± 5.91
1.5	1.27	2.512	12	4.78 ± 1.38	4.712	42.16 ± 8.79
2.2	1.88	3.308	9	2.72 ± 0.91	10.493	70.70 ± 12.98

stars employed in Dobbie et al. (2002b). The majority of these stars were originally drawn from the recent 2MASS survey and hence observed K photometry has been obtained from the SIPSC. We find that the transform between the two systems is described by the equation $I_C - I_{KP} = 0.049(I_{KP} - K) + 0.069$ $(2.3 \leqslant I_{KP} - K \leqslant 5.8)$. The typical differences are found to be consistent with the values derived from Bessel (1986) using his diagram of $I_C - I_{CCD}$ as a function of $R - I$. We have therefore converted the Pinfield et al. (2000) photometry to Cousins using this equation, though preferring other estimates of I_C (e.g. from the CFHT, ITP or IWFC surveys) where they exist.

3 INFRARED PHOTOMETRY OF CANDIDATE CLUSTER MEMBERS

Contamination in the optical colour–magnitude (I–Z and R–I) diagrams is rather uncertain. Martín, Rebolo & Zapatero-Osorio (1996) present spectroscopic follow-up of a deep RI CCD survey (Zapatero-Osorio et al. 1997a) and find that only 50 per cent of their colour–magnitude selected candidates are likely cluster members, the remainder being field M-type dwarfs. Moraux et al. (2001) find the level of contamination in the CFHT survey to be 31 per cent, close to the Bouvier et al. prediction of 25 per cent which was based on the field-star luminosity function as determined from the DENIS survey.

All four surveys have removed or flagged extended (i.e. likely galaxy) contaminants. A further problem for the ITP, Burrell Schmidt and IWFC surveys is the small colour baseline of the IZ filter combination. The cluster sequence is not as well separated from the field as one would find with longer-baseline colours such as I–K. Thus, especially towards the limit of the survey where photometric errors become significant ($\Delta I = 0.15$ mag at $I = 22$), one may expect a number of objects that are really below the sequence to appear red enough to be included in the sample.

Before we can accurately determine the luminosity and mass functions of the Pleiades, it is crucial to weed out the bulk of these contaminants. Dobbie et al. (2002a), Pinfield et al. (2000), Hodgkin et al. (1999) and Zapatero-Osorio, Martín & Rebolo (1997b) have shown that an additional measurement at K provides an efficient test for cluster membership in the absence of spectroscopy and proper motions.

3.1 IR observations

Our K-band photometry for the IWFC and BPL candidates has been published by Dobbie et al. (2002a) and Pinfield et al. (2000), respectively. We also supplement the K-band photometry of Pinfield et al. (2000) with some improved measurements taken from Pinfield et al. (2002, in preparation). K- (and some J- and H-) band photometry were obtained for the bulk of ITP candidates and the probable BDs of the CFHT survey using United Kingdom Infrared Telescope (UKIRT) and the IRCAM3 instrument. The data were acquired during photometrically-good periods on the nights 1997 November 26 to December 2 and 1998 November 14–15. IRCAM3 is a 256×256 pixel InSb array which for the course of these observing runs was employed with the J_{Barr}, H_{Barr} and K_{Ocli} filters. Each candidate was observed for a total of between 150 and 300 s, depending on the I magnitude, initially at K, and where a candidate appeared to be on or near to the Pleiades sequence also at J and H. A five-point dither pattern was used throughout, placing the star on a different part of the detector for each of five sub-exposures. This enables accurate flatfielding by using the median of each pixel to derive a sky flat for each target.

All data reduction (dark subtraction, flatfielding) was performed within the STARLINK IRCAMDR package. Instrumental magnitudes were also measured using the IRCAMDR package. Photometric errors for the targets were derived from the scatter in each of the five subexposures. To calibrate the JHK photometry observations of UKIRT, faint standards (from the list of Casali & Hawarden 1992) were obtained each night at a variety of airmasses. The typical residuals in the airmass curves for the nights in question were found to be $\sim$0.02 mag. These were quadratically combined with the photometric errors to provide an estimate of the overall uncertainty. Subsequently, the photometry was transformed onto the Mauna Kea Observatories (MKO) system using the equations of Hawarden et al. (2001). Where no J photometry was available, a colour of J–$K = 1.0$ was assumed, which is appropriate to objects of mid- to late-M spectral type (e.g. Kirkpatrick et al. 1999). Our MKO magnitudes and corresponding uncertainties for the brown dwarf candidates are presented in Table 1. We find that, where available for candidates, previously published infrared data (e.g. Martín et al. 2000) are largely consistent with this photometry.

3.2 Selection of low-mass Pleiads from the *IK* CMD

The I_C, I_C–K_{MKO} (hereafter I, I–K) CMD for the bulk of the ITP candidates is shown in Fig. 1. Candidate Pleiades BDs from the CFHT, BPL and IWFC surveys are shown as filled circles. Overplotted are the NEXTGEN and DUSTY model isochrones for solar metalicity and ages of 125 and 120 Myr, respectively (Baraffe et al. 1998; Chabrier et al. 2000). As was done in Dobbie et al. (2002a), these have been offset with a distance of $(m - M)_0 = 5.53$ (Crawford & Perry 1976) and modified for an extinction of $A_I = 0.07$ and a reddening of $E(I - K = 0.06)$ (Fitzpatrick 1999). We note that for objects of late-M spectral type, $K_{CIT} = K_{MKO}$.

The strengths of the Lyon group's models include a detailed and self-consistent full non-grey treatment of the stellar atmosphere. In contrast, the models of other theoretical groups (e.g. D'Antona

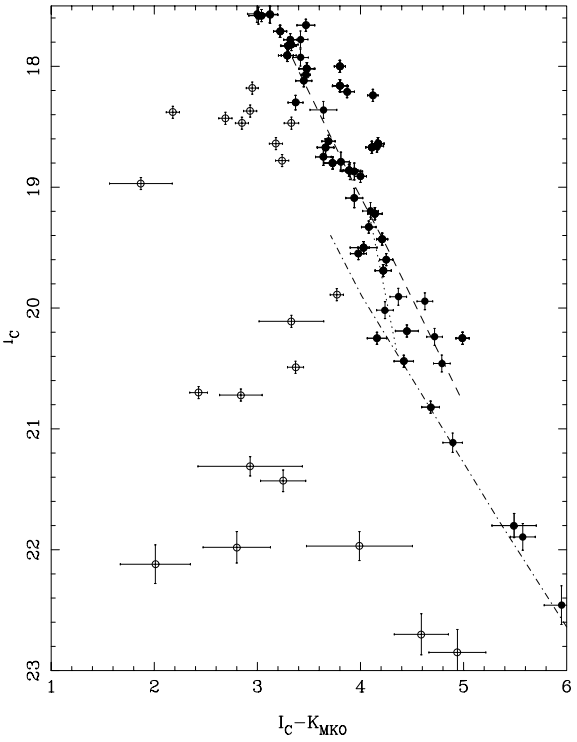

Figure 1. An *I*–*K* colour–magnitude plot of candidate low-mass Pleiads from the four optical surveys. Candidates drawn from the CFHT, BPL and IWFC surveys and ITP candidates found here to have *I*–*K* colours consistent with cluster membership are represented by filled circles; ITP candidates deemed non-members are represented by open circles. The NEXTGEN (125 Myr; dashed line) and DUSTY (120 Myr; dot–dashed line) theoretical isochrones of Baraffe et al. (1998) and Chabrier et al. (2000), respectively, are also shown. Our estimated location of the cluster sequence in the range $19.2 < I < 20.4$ is shown by the dotted line.

& Mazzitelli 1997; Burrows et al. 1993, 1997) employ, to some degree, simpler grey approximations at this outer boundary which in addition to differences in the treatment of convection leads to the overestimation of $T_{\rm eff}$ and luminosity at a given mass (e.g. see Baraffe et al. 2002; Chabrier & Baraffe 1996; D'Antona & Mazzitelli 1997). The detailed treatment of the atmosphere also means that the Lyon models directly predict the flux in the relevant photometric bands. Hence they do not rely on the application of uncertain bolometric corrections and temperature–colour relationships to be transformed onto the observational plane as do the other evolutionary models. Furthermore, the Lyon group models have been found to be most successful in predicting coeval ages for the different mass components in the young multiple system GG Tau (White et al. 1999). The atmospheres used in the DUSTY models, unlike those used in the NEXTGEN calculations, include a treatment for the formation in cool stellar atmospheres of dust grains: at $T_{\rm eff}$s that correspond to late-M and early-L spectral-types, species such as TiO and VO begin to condense into dust grains, reducing the level of opacity in the *I* band and resulting in objects having bluer *I*–*K* colours than predicted by the NEXTGEN models.

A glance at the *I*, *I*–*K* CMD reveals a distinct cluster sequence down to $I \sim 19.2$, approximately the completeness limit of the BPL and CFHT surveys. The level of agreement between the locations of the observed sequence at $I \lesssim 19.2$ and the NEXTGEN isochrone is most satisfying. The cluster binary sequence is also clearly seen in the upper quarter of this plot, sitting 0.75 above the single-star sequence. However, this appears to truncate at I–$K \sim 4.2$. A rather less obvious cluster sequence continues at fainter magnitudes ($I_{\rm C} \gtrsim 20.5$), the location of which is rather well matched by the DUSTY isochrone. We note also a number of sources clumped around $I \sim 20.2$, I–$K \sim 4.8$, approximately 0.75 mag above the DUSTY isochrone. We suggest that the observed features of the CMD can be explained if the *I*, *I*–*K* isochrone steepens dramatically at around I–$K \sim 4.0$–4.4 as dust begins to exert an influence on the *I*–*K* colour. The cluster sequence then turns back towards the red at $I \gtrsim 20.4$, following the DUSTY model predictions quite closely. We have indicated the likely form of the sequence from $I = 19.2$–20.4 with a dotted line in Fig. 1. In this interpretation, the single and binary star sequences would appear to merge between $19.2 \lesssim I \lesssim 19.8$. The clump of objects discussed above would represent the binary sequence after demerging from the single-star sequence.

To select candidate cluster members from the *I*, *I*–*K* CMD once again, we opt to follow closely the arguments of Dobbie et al. (2002a). We use the NEXTGEN isochrone as a guide for $I \lesssim 19.2$, the DUSTY isochrone for $I \gtrsim 20.4$ and our dotted line between these limits. In addition we take into account uncertainties in the age and the distance of the cluster and the effect of the cluster depth (± 0.2 mag). The likely extremes of the age of the cluster (70–150 Myr) result in a displacement of the theoretical substellar sequence by ~ -0.3 and $\sim +0.1$ mag, respectively. Different distance estimates result in a displacement of ~ -0.2 (*Hipparcos*) and $\sim +0.1$ (photometry). An additional factor that must be taken into account here is the presence of unresolved binaries which may lie up to 0.75 mag above the single-star sequence (e.g. Steele & Jameson 1995). Accounting for all these uncertainties and allowing for a small degree of error in both the theoretical models and the transforms, we choose to select all candidates lying no more than 0.3 mag below and no more than 1.0 mag above the single-star sequence. In this way we identify 20 of the ITP candidates as probable low-mass Pleiades members. These are also shown in Fig. 1 as filled circles. The infrared photometry of Zapatero-Osorio (private communication) indicates that the 4 ITP candidates we were unable to observe (Roque 34, Roque 32, Roque 18 and Roque 2) all lie well below the cluster sequence and do not need to be considered further here. Reassuringly, all 11 of the CFHT candidates that have proper motions consistent with cluster membership (Moraux et al. 2001) are also recovered here as probable cluster members. A summary of the adopted membership status of the candidate low-mass Pleiads originally proposed by the four optical surveys is given in Table 2.

3.3 Residual contamination in our definitive list of low-mass Pleiads

As determined by previous studies of the Pleiades which used colour to select candidate members (e.g. Zapatero-Osorio et al. 1997a; Festin 1997), late-type field stars are likely to be the greatest source of contamination in our refined candidate list. Estimates of the level

Table 2. Our estimated values for the Pleiades luminosity and mass functions in the substellar regime.

Mag. bin ($I_{\rm C}$)	Mass bin ($M_\odot$)	$\bar{m}$ ($M_\odot$)	$N_{\rm total}$	n per 0.1 $M_\odot$
17.80–19.50	0.074−0.050	0.062	100^{+11}_{-20}	417^{+46}_{-83}
19.51–21.90	0.050−0.033	0.042	102^{+37}_{-37}	600^{+218}_{-218}

of contamination from background giants in such surveys indicate that this is less than that of late-type dwarfs by a factor of a few while as discussed earlier the four optical surveys have flagged or removed extended objects, eliminating the bulk of contaminating galaxies. However, given the rather mixed nature of the criteria which have been used either to include or exclude candidates in our list (spectroscopy, photometry, proper motions) we can only provide an approximate estimate of the number of residual late-type field-star contaminants.

We note that the combined surveys are sensitive to spectral types ∼M6–L1 over the magnitude range for which the luminosity function is to be derived ($17.8 \leqslant I \leqslant 21.9$). The models of Baraffe et al. (1998) indicate that, owing to their youth, Pleiades members in this range are overluminous with respect to field stars of similar spectral type by approximately 1 mag. If candidates are selected solely on the criterion that they lie within 0.3 and 1.0 mag on the low and high side of the I, I–K theoretical isochrone, respectively, then the survey is sensitive to single and binary field dwarfs between 51–92 and 72–131 pc, respectively (assuming equal-mass binaries). With a total area surveyed of 7.6 square degrees, allowing for overlap between the surveys, this corresponds to space volumes of 497 and 1444 pc^3 for single and binary field stars, respectively. However, the BD candidates taken from the CFHT survey (Moraux et al. 2001) and from the bright end of BPL survey ($I \leqslant 18.3$) have, in addition to I–K colour, been discriminated on the grounds of their proper motion. Assuming that contamination by field stars in a sample selected by both proper motion and I–K colour is negligible, then only the IWFC and ITP surveys are likely to contribute a significant number of M6–M7 field-star interlopers. From fig. 14 of Kirkpatrick et al. (1994) we estimate a space density of ≈ 0.0025 pc^{-3} for objects of this type. Thus we estimate that in this range ($17.8 \leqslant I \leqslant 18.3$ M6–M7), the 2.1 square degrees covered by the IWFC and ITP surveys contributes ∼1 field-star interloper to the refined list. Over the range $18.3 < I \leqslant 19.5$ (M7.5–M8.5) candidates were selected from an area of 5.1 square degrees largely on the basis of I–K colour alone (i.e. the BPL, IWFC, ITP surveys). Again drawing from Kirkpatrick et al. (1994), we similarly estimate a space density of ≈ 0.0025 pc^{-3} for objects of this type, which should contribute ∼2 field-star interlopers to our refined list of members. Only the ITP and IWFC surveys covering 2.1 square degrees are complete up to fainter magnitudes, probing spectral types M9–L1. Gizis et al. (2000) estimate the space densities of field objects of spectral types M9–M9.5 and L0–L4.5 to be 0.0026 and 0.002 pc^{-3}, respectively. Combining these values, we estimate the space density of M9–L1 objects to be 0.0035 pc^{-3}. This gives an additional contamination of ∼2 late-type field stars. Thus of all the candidate brown dwarfs included in our subsequent analyses we estimate that ∼10 per cent are likely non-members.

4 THE CLUSTER CORE RADIUS FOR BROWN DWARFS

4.1 Defining a magnitude-limited sample of Pleiades brown dwarfs

In order to analyse the spatial distribution of Pleiades BDs, we must confine ourselves to a well-defined and complete sample. A BD of solar metalicity (and the Pleiades metalicity is approximately solar), should have a mass <0.075 $M_\odot$ (Baraffe et al. 1998). However, mass is not a directly observable quantity. It has been shown that for the age of the Pleiades this mass corresponds closely to the boundary where the lithium 6707-Å line reappears in the spectrum (e.g. Basri, Marcy & Graham 1996). Stauffer, Schultz & Kirkpatrick (1998) measure spectra for some eight low-mass Pleiads and find the Lithium boundary at $I = 17.8$ (I_C), corresponding to a Pleiades age of 125 ± 8 Myr. We therefore adopt the lithium boundary as a working definition of a Pleiades BD and as a suitable bright limit. Secondly, the least-sensitive surveys (the BPL and the CFHT) impose a faint completeness limit of $I \leqslant 19.5$. We imposed these selection criteria on the candidates from the four surveys and produced the list of 32 BDs shown in the upper section of Table 3. For completeness, in the lower section of Table 3 we list 16 additional candidate BDs primarily from the two deeper surveys (ITP and IWFC) most of which have been included in the calculation of the luminosity and mass functions (see Section 5).

4.2 Fitting the cluster profile

It is important to know the spatial distribution of the Pleiades stars as a function of their mass in order properly to determine the luminosity and mass functions for the cluster. Pinfield et al. (1998) show that the cluster stars can be well fitted by a King distribution (King 1962) whose core radius increases as the stellar mass decreases. In this section we shall again assume a King distribution and try to find the core radius applicable for BDs. Equation (1) shows the King surface density distribution:

$$f = k\left[\frac{1}{\sqrt{1+x}} - \frac{1}{\sqrt{1+x_t}}\right]^2, \qquad (1)$$

where $x = (r/r_c)^2$ and $x_t = (r_t/r_c)^2$, with r the radius from the cluster centre, r_c the core radius and r_t is the tidal radius of the cluster, where the gravitational potential from the galaxy equals the cluster potential. We take $r_t = 5.54^\circ$ parsecs after Pinfield et al. (1998). f is therefore the stellar density at a radius r, and k is the normalization constant.

$$n(x) = \pi r_c^2 k\left[\ln(1+x) - 4\frac{\sqrt{1+x}-1}{\sqrt{1+x_t}} + \frac{x}{1+x_t}\right] \qquad (2)$$

Equation (2) is the cumulative King distribution, obtained by integrating equation (1) with respect to $2\pi r\ \mathrm{d}r$. It gives the total number of stars in projection within a distance r of the centre of the cluster. The spatial distribution of our magnitude-limited sample of Pleiades BDs is shown in Fig. 2 together with rectangles to represent the areas of the cluster included in the four optical surveys. Overplotted are circles of radii 1.0, 1.5 and 2.2 degrees (corresponding to 2.23, 3.35 and 4.92 parsecs) centred on RA 03^h47^m Dec. $+24^\circ07'$, J2000.0 (Pinfield et al. 1998). From this diagram we determined the area surveyed within the central circle and annuli (allowing for any overlap between the surveys) and the number of BDs found therein. We then obtained radial surface densities by dividing the numbers of BDs in any annulus by the surveyed area and inferred the total number of magnitude-limited BDs in each annulus by multiplying this surface density by the total annulus area. The results are given in Table 4 where the errors are from counting statistics.

The surface density and cumulative number of magnitude-limited BDs as a function of radial distance are plotted in Figs 3(a) and 3(b), respectively. Using equations (1) and (2) and a tidal radius of 5.54° (Pinfield et al. 1998), we use a χ-squared minimization technique (DXSRCHMIN) (R. Willingale) to fit for r_c and k. We found $k = 19.67^{+2.04}_{-2.91}$ per square degree and $r_c = 2.22^{+1.36}_{-0.67}$ degrees (or $5.0^{+3.0}_{-1.5}$ pc at Pleiades distance). We also obtain an integrated total of 100^{+11}_{-20} BDs in our magnitude-limited range.

The core radii for stellar members, from Pinfield et al. (1998), together with our BD core radius point are shown in Fig. 4. Pinfield,

Table 3. *IZJHK* photometry for ITP and CFHT brown dwarf candidates.

ITP name	I_C	Z_{RGO}	J_{MKO}	±	H_{MKO}	±	K_{MKO}	±	IR ref.[a]	Cross IDs[c]	Photometric member?	Comments
Roque 48	17.58	16.75					14.54	0.04	U		√	
HHJ 3	17.66	16.62	15.16	0.10	14.64	0.09	14.19	0.07	U		√	
Roque 47	18.12	17.12					14.67	0.06	U	IPMBD 20	√	I_C(IPMBD) = 18.05
Roque 16	18.12	17.10	15.51	0.11	14.99	0.09	14.62	0.03	U,p02	CFHT-PL-11, BPl 152	√	I_C(CFHT) = 17.91
Roque 15	18.21	17.09	15.37	0.08	14.82	0.06	14.34	0.05	U	PPl 1	√	
Roque 17	18.16	16.97	15.31	0.09	14.79	0.07	14.36	0.05	U,p02	BPl 142, INT-PL-IZ-37	√	
Roque 46	18.18	17.36					15.23	0.03	U		×	
PPl 15	18.24	17.02	15.34		14.77		14.41	0.03	b96,h99	NPL 35, IPMBD 23	√	I_C(NPL) = 17.91
Roque 44	18.37	17.50					15.44	0.04	U		×	
Roque 42	18.43	17.60					15.74	0.04	U		×	
Roque 40	18.38	17.68					16.20	0.04	U		×	
Roque 41	18.47	17.61					15.62	0.04	U		×	
Roque 43	18.47	17.38	16.07	0.10	15.57	0.08	15.14	0.05	U	JS 1, PPl 3	×	
Roque 14	18.64	17.42	15.53	0.10	14.96	0.09	14.47	0.03	U,p02	BPl 108	√	
Roque 13	18.67	17.47	15.65	0.09	15.11	0.08	14.56	0.03	U,p02	BPl 79	√	
Roque 38	18.64	17.65					15.46	0.04	U		×	
Roque 12	18.86	17.78	15.93	0.10	15.44	0.08	14.97	0.07	U	NPL 36, BPl 172	√	I_C(NPL) = 18.66
Roque 37	18.78	17.79	16.50	0.10	15.89	0.05	15.54	0.04	U		×	
Teide 1	19.22	17.90	16.19	0.11	15.65	0.09	15.08	0.05	U	NPL 39, BPl 137	√	I_C(NPL) = 19.26
Roque 10[b]	18.97	17.99					17.1:	0.3	U		×	
Roque 9	19.43	18.26	16.30	0.19	15.72	0.15	15.22	0.02	U	BPl 100	√	
Roque 8	19.55	18.24	16.68	0.11	16.14	0.10	15.57	0.06	U		√	
Roque 7	19.74	18.50	16.55	0.18	15.88	0.14	15.47	0.02	U	BPl 62, CFHT-PL-24	√	I_C(CFHT) = 19.50
Roque 6	19.89	18.75					16.12	0.04	U		×	
Roque 5	20.19	18.90	16.89	0.14	16.33	0.15	15.74	0.10	U		√	
Roque 4	20.25	18.97	16.69	0.12	16.04	0.09	15.26	0.04	U,p02	BPl 66	√	
Roque 3	20.11	19.01	17.8:	0.4	17.2:	0.4	16.8:	0.3	U		×	
Roque 36	20.25	19.02	17.17	0.20	16.58	0.12	16.09	0.08	U		√	
Roque 33	20.44	19.06	17.07	0.12	16.62	0.18	16.02	0.08	U	NPL 40	√	I_C(NPL) = 20.55
Roque 31	20.49	19.33					17.12	0.06	U		×	
Roque 30	20.82	19.45	17.49	0.12	16.77	0.11	16.14	0.07	U		√	
Roque 29	20.72	19.65					17.9:	0.2	U		×	
Roque 28	20.70	19.62	18.64	0.12			18.27	0.07	U		×	
Roque 27	21.31	20.06					18.38	0.5	U		×	
Roque 26	21.43	20.12					18.18	0.2	U		×	
Roque 25	21.80	20.14	17.7:	0.3	17.0:	0.3	16.31	0.19	U		√	
Roque 24	21.97	20.36					18.0:	0.5	U		×	
Roque 23	21.98	20.61					19.2:	0.3	U		×	
Roque 22[b]	22.1:	20.70					20.1:	0.3	U		×	
Roque 20	22.2:	21.10							U		×	No source at *K*
Roque 21[b]	22.7:	21.10					18.1:	0.2	U		×	
Roque 19[b]	22.9:	21.10					17.9:	0.2	U		×	
CFHT-PL-9	17.71						14.49	0.04	U	BPl 202	√	
CFHT-PL-10	17.82						14.49	0.04	U		√	
CFHT-PL-12	18.00						14.20	0.02	U,p02	BPl 294	√	
CFHT-PL-13	18.02		15.49	0.08	14.97	0.07	14.54	0.06	U	Teide 2, BPl 254	√	
CFHT-PL-15	18.62						14.93	0.04	U		√	
CFHT-PL-16	18.66						14.50	0.04	U		√	
CFHT-PL-17	18.80		16.14	0.10	15.51	0.11	15.07	0.07	U	BPL 49	√	
CFHT-PL-23	19.33		16.38	0.08	15.79	0.08	15.25	0.05	U		√	
CFHT-PL-25	19.69		16.64	0.15	16.05	0.13	15.47	0.06	U,p02	BPl 303	√	

[a] U: UKIRT; b96: Basri, Marcy & Graham (1996); h99: Hambly et al. (1999); p02: (Pinfield et al. 2002, in preparation).
[b] Objects appear slightly extended in *I Z* images.
[c] PPl objects, Stauffer, Hamilton & Probst (1994); JS objects, Jameson & Skillen (1989); NPL objects, Festin (1998); IPMBD objects, Hambly et al. (1999).
:Large uncertainties in photometry. For details of uncertainties in *I Z* photometry see Zapatero-Osorio et al. (1999).

Jameson & Hodgkin (1998) found that the core radius varied with stellar mass as $m^{-0.5}$, as expected for a dynamically-relaxed cluster, but noted a possible levelling-off of the core radius at 1.23° in their lowest-mass bin (0.3 $M_\odot$). A study of the spatial distribution of a small sample of Pleiades BD candidates seemed to support this unexpected finding and even suggest that the relationship turned over at the very-lowest (substellar) masses (Jameson et al. 1999). As the estimated time-scale on which dynamical relaxation occurs in the Pleiades is comparable to the 125 Myr cluster age, it was proposed that while the high-mass Pleiads were dynamically relaxed

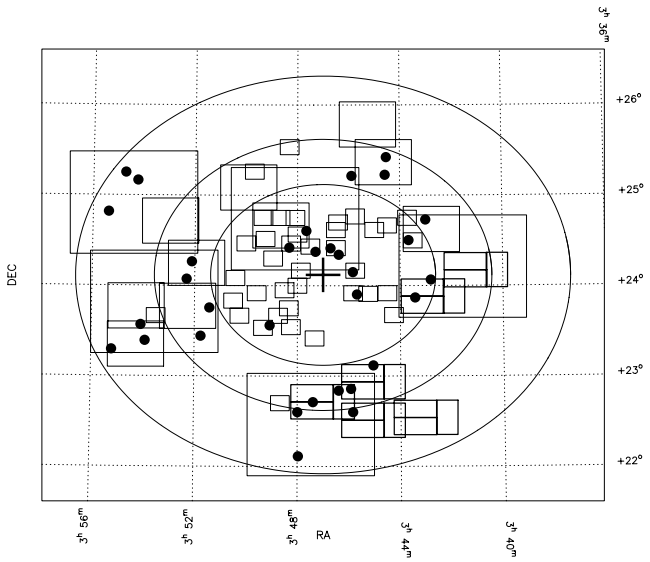

Figure 2. Plot showing the spatial distribution of candidates ($I \leqslant 19.5$; heavy black dots). Overplotted are the outlines of the areas covered by the four optical surveys and circles of radii 1.0°, 1.5° and 2.2°.

the lowest-mass members of the cluster may not yet have reached this state of equilibrium.

At variance with the findings of this previous study, which used fewer BD candidates, Fig. 4 indicates that the core radius does not turn over or level off at substellar masses. Indeed, our new result is consistent with a continuation of the relationship observed for the higher-mass members suggesting instead that the lowest-mass members are also in a state of dynamical relaxation. However, given the large errors on our estimate of r_c for the BDs our result can also be consistent with a moderate flattening of the relationship at $M < 0.5\ M_\odot$ and we are unable to exclude the possibility that the lowest-mass members may be only partially relaxed. Alternatively, some degree of flattening might be expected because of the evaporation from the cluster of low-mass members in the high-velocity tail of the equilibrium distribution. Either way, the result presented here is important; an incorrect core radius for the BDs will result in erroneous estimates of the cluster luminosity and mass functions in the substellar regime.

5 STRINGENT CONSTRAINTS ON THE MASS FUNCTION OF THE PLEIADES

In Section 4.3 our fitted cluster profile implies that there are 100^{+11}_{-20} Pleiades brown dwarfs in the magnitude range $17.8 \leqslant I \leqslant 19.5$. However, Table 3 contains details of a further 16 candidate BDs with $I > 19.50$. Of these, 14 unearthed by the deeper ITP and IWFC surveys have also been used to determine the cluster mass function. We did not consider BPL303 (CFHT-PL-25) in this analysis as it was unearthed by the Burrell Schmidt and CFHT surveys, which are not complete at the magnitude of this source. Furthermore, we excluded INT-PL-IZ-69 as it is fainter than the 90 per cent completeness limit of the ITP survey, which we estimate to occur at $I = 21.9$. The positions of the fainter candidates used in the mass function analysis are shown in Fig. 5.

Using the same approach as we used for the brighter sample, we counted up the number observed in the central circle and annuli and scaled this up to the number expected in the whole region. Subsequently, we summed up the candidates to determine the cumulative number out to 2.2°. We then assumed that $r_c = 2.22°$ and used equation (2) to determine the ratio $n(r_t)/n(r = 2.2°)$, which we used to extrapolate the cumulative counts out to the tidal radius. The results are given in Table 5. The quoted uncertainties in the faintest luminosity function point are dominated by counting statistics.

As the DUSTY model provides a systematically lower estimate of mass, we have adopted the more conservative NEXTGEN model to derive the mass boundaries of the luminosity bins. In this way we calculated the values of the mass function, dN/dM (0.1 $M_\odot$). Our results are given in the final column of Table 2 and can be seen plotted in Fig. 6. Adams et al. (2001) have recently made a large-scale survey of the entire Pleiades cluster for stars of mass 1.0–0.1 $M_\odot$. We include in Fig. 6 their estimated mass function and best-fit log-normal function with which they model their points. It is gratifying to note that the stellar and BD mass functions fit together quite smoothly. The combined result we believe represents the best mass function yet obtained for the Pleiades. Using a χ-squared minimization technique we fitted a power law to the four lowest-mass bins ($0.3\ M_\odot \gtrsim M \gtrsim 0.035\ M_\odot$) and derived an index of $\alpha = 0.41 \pm 0.08$, where the quoted uncertainty is the formal 1σ fit error.

To determine the robustness of this result first we examine its sensitivity to uncertainties in the cluster age. Assuming an age of 70 Myr and using the NEXTGEN models, we calculated mass function points of 526^{+58}_{-105} and 729^{+212}_{-212} for mass bins $0.057 - 0.038$ and $0.038 - 0.024\ M_\odot$, respectively, which resulted in a best-fit power law that has a slightly steeper index of $\alpha = 0.48 \pm 0.07$. Note that in this case and each of the following we do not modify the mass function points from Adams et al. (2001). Assuming an age of 150 Myr we obtain mass function points of 385^{+42}_{-76} and 567^{+165}_{-165} for mass bins $0.08 - 0.054$ and 0.054–0.036 $M_\odot$, respectively. In this case the best-fit power law has a slightly shallower index of $\alpha = 0.37 \pm 0.08$.

Next we examine the sensitivity to the choice of theoretical model. By employing the DUSTY model we derived mass function points of 526^{+58}_{-105} and 729^{+212}_{-212} for mass bins $0.057 - 0.038$ and 0.038–0.024 $M_\odot$, respectively, giving a best-fit power-law index

Table 4. Summary details of the four optical surveys employed here: in column 2 the area covered by each, in column 3 the estimated depth to which each is complete, in column 4 the total number of candidate low-mass stellar and substellar Pleiades originally unearthed by each survey, in column 5 the total number of candidates from each survey determined to have $I_C \geqslant 17.8$, i.e. BD candidates, in column 6 the number of candidate BDs adopted here as members, in column 7 the number of candidate BDs rejected here as non-members, and finally in column 8 the number of BDs from each survey duplicated in the surveys listed previously.

Survey	Area surveyed (sqr.°)	Depth to which compete (I_C)	Total no. of candidates	Total no. of candidate BDs ($I_C \geqslant 17.8$)	No. adopted here as BDs	No. rejected here as BDs	No. of BDs duplicated
ITP	1.1	∼21.5	47	45	17	28	na
CFHT	2.5	∼19.5	26	17	11	6	2
BPL	6.4	∼19.5	309	27	23	4	13
IWFC	1.1	∼22.0	23	16	16	0	4

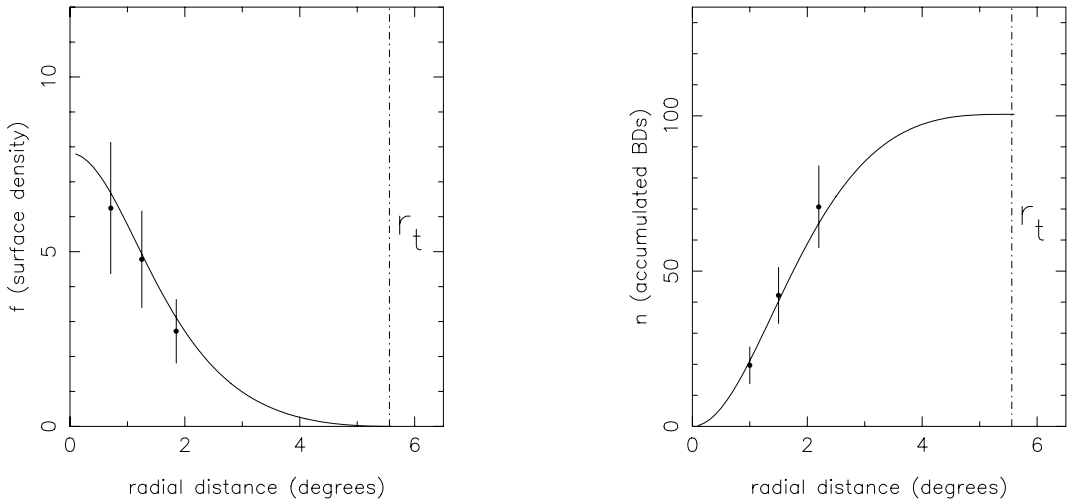

Figure 3. (a) BD surface density as a function of radial distance from the cluster centre. Overplotted is the best-fitting King profile, details of which are given in the text. (b) Cumulative number of BDs as a function of radial distance from the cluster centre. Overplotted is the best-fitting King profile, details of which are given in the text.

of $\alpha = 0.51 \pm 0.07$. With the D'Antona & Mazzitelli (1997) model, where we have used the colour–$T_{\rm eff}$ relationships and bolometric corrections of Bessell, Castelli & Plez (1998), the mass function points are 588^{+65}_{-117} and 927^{+269}_{-269} for mass bins 0.057–0.038 and 0.038–0.024 $M_\odot$, respectively. This results in a best-fit power-law index of $\alpha = 0.59 \pm 0.07$. Finally, using the Burrows et al. (1993) model we calculated mass function points of 435^{+48}_{-87} and 927^{+269}_{-269}, respectively, producing a best-fit power law with index $\alpha = 0.45 \pm 0.07$. Hence only the index derived using the D'Antona & Mazzitelli (1997) model is found to be significantly different from the estimate obtained using our preferred model, and even this discrepancy is marginal. We also find our result to be largely insensitive to plausible uncertainties in the distance of the cluster, as concluded earlier in Section 4.3. For example, assuming a smaller cluster distance of $(m - M)_0 = 5.35$ we calculate mass function points of 455^{+50}_{-91} and 637^{+185}_{-185} in the mass bins 0.07–0.048 and 0.048–0.032 $M_\odot$, respectively. The best-fitting power law to the four lowest-mass points is then $\alpha = 0.45 \pm 0.08$.

The binary fraction of substellar Pleiads would also affect the shape of the CMF but is currently not well known. Steele & Jameson (1995) have estimated the binary fraction of low-mass stellar members to be ∼46 per cent. Assuming a similar fraction of the candidate members listed here to be equal-mass binaries, we determine the index of the best-fit power law to be $\alpha = 0.50 \pm 0.08$. Moraux et al. (2001) found a similar steepening of their best-fit power law by treating as equal-mass systems those CFHT candidates suspected of being unresolved binaries from their location in the CMD. Hence our result does not appear to be unduly sensitive to the presence of unresolved binaries.

Our result agrees well with the $\alpha = 0.51 \pm 0.15$ index obtained over the range $0.35\ M_\odot \gtrsim M \gtrsim 0.05\ M_\odot$ from the CFHT survey

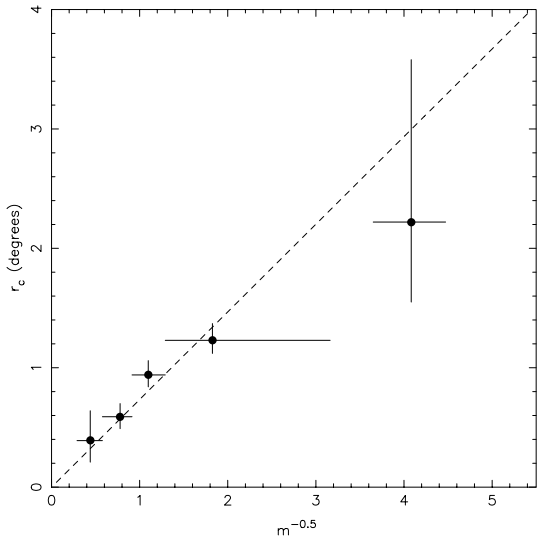

Figure 4. Plot of core radius as a function of $m^{-0.5}$. The four leftmost points are taken from Pinfield et al. (1998). The point corresponding to the lowest masses is derived here. The dashed line represents the relationship $r_c = 0.733 m^{-0.5}$.

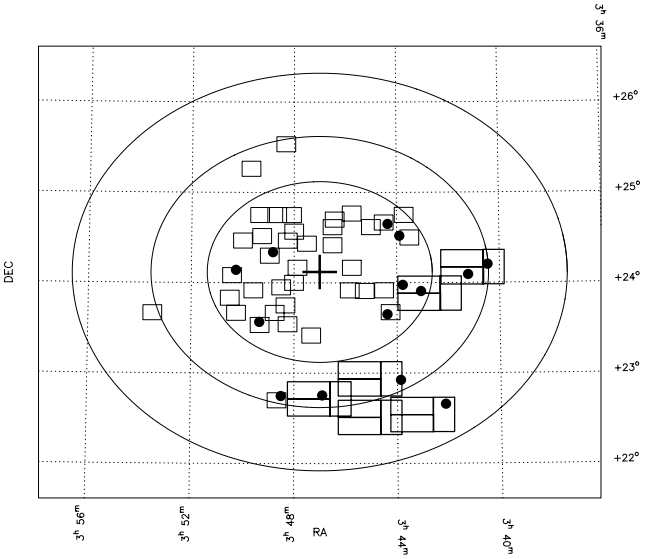

Figure 5. Plot showing the spatial distribution of candidate BDs (heavy filled circles) in the magnitude range $19.50 < I_C \leqslant 21.90$.

Table 5. IJHK photometry for our compilation of Pleiades BDs. Excluding those objects shown in italics, this is a complete magnitude-limited sample ($17.8 \leqslant I \leqslant 19.5$).

Name													
Burrell	CFHT	ITP	IWFC	NOT	Schmidt	Other	I_C	J	H	K	I ref.[a]	IR ref.[a]	Notes
	CFHT-PL-10						17.82			14.49	C	U	μ[1]
BPL163							17.83			14.53	B	p02	
BPL58			INT-PL-IZ-6				17.83			14.53	D	D	
			INT-PL-IZ-42				17.84			14.36	D	D	
BPL152	CFHT-PL-11	Roque 16					17.91	15.51	14.99	14.62	C	U,p02	Li[2], μ[1,3]
			INT-PL-IZ-60				17.99			14.51	D	D	
BPL294	CFHT-PL-12						18.00			14.20	C	p02	Li[2], μ[1,3]
BPL254	CFHT-PL-13					Teide 2	18.02	15.49	14.97	14.54	C	U	Li[2,4], μ[1]
BPL327					IPMBD11		18.07			14.60	H	p02	μ[5]
		Roque 47			IPMBD20		18.12			14.67	I	U	$I_C = 18.05$[5]
BPL142		Roque 17	INT-PL-IZ-37				18.16	15.31	14.79	14.36	I	U,p02	
		Roque 15				PPL 1	18.21	15.39	14.74	14.34	I	U	Li[2]
				NPL 35	IPMBD23	PPL 15	18.24	15.34	14.65	14.41	I	b96,h99	Li[6]
BPL316							18.30			14.93	B	p02	μ[3]
			INT-PL-IZ-43				18.41			14.70	D	D	
	CFHT-PL-15						18.62			14.93	C	U	Li[2], μ[1]
BPL108		Roque 14					18.64	15.53	14.96	14.47	I	U,p02	
	CFHT-PL-16						18.66			14.50	C	U	μ[1]
BPL78			INT-PL-IZ-44				18.67			15.01	D	p02	
BPL79		Roque 13					18.67	15.65	15.11	14.56	I	U,p02	Li[2]
BPL240							18.75			15.11	B	p02	
BPL81							18.79			14.98	B	p02	
BPL49	CFHT-PL-17						18.80	16.14	15.51	15.07	C	U	μ[1]
BPL172		Roque 12		NPL 36			18.86	15.93	15.44	14.97	I	U	$I_C = 18.66$[7]
BPL45			INT-PL-IZ-29				18.87			14.93	D	p02	
BPL235	CFHT-PL-21					Calar 3	19.00	16.29	15.45	14.91	C	U,p02	Li[8], μ[1]
BPL306							19.09			15.15	B	p02	
BPL137				NPL 39		Teide 1	19.22	16.19	15.65	15.08	I	U,p02	Li[8], μ[9]
			INT-PL-IZ-33				19.23			15.10	D	D	
	CFHT-PL-23						19.33	16.38	15.79	15.25	C	U	μ[1]
BPL100		Roque 9					19.43	16.32	15.64	15.22	I	U	
BPL62	CFHT-PL-24	Roque 7					19.50	16.55	15.88	15.47	C	U	μ[1]
					$19.5 < I \leqslant 21.9$								
		Roque 8					19.55	16.68	16.14	15.57	I	U	
BPL303	*CFHT-PL-25*						*19.69*	*16.64*	*16.05*	*15.47*	*C*	*p02*	
			INT-PL-IZ-48				19.93			15.54	D	D	
			INT-PL-IZ-76				19.96			15.32	D	D	
			INT-PL-IZ-55				20.04			15.78	D	D	
		Roque 5					20.19	16.89	16.33	15.74	I	U	
			INT-PL-IZ-25				20.25			15.52	D	D	
		Roque 36					20.25	17.17	16.58	16.09	I	U	
BPL66		Roque 4					20.25	16.69	16.04	15.26	I	U,p02	
		Roque 33		NPL 40			20.44	17.07	16.62	16.02	I	U	$I_C = 20.55$[7]
			INT-PL-IZ-20				20.47			15.67	D	D	
		Roque 30					20.82	15.49	16.77	16.14	I	U	
			INT-PL-IZ-84				21.12			16.22	D	D	
		Roque 25					21.80	17.7	17.0	16.31	I	U	
			INT-PL-IZ-81				21.87			16.32	D	D	
			INT-PL-IZ-69				*22.46*			*16.51*	*D*	*D*	

[a] C: CFHT; I: ITP; B: Burrell Schmidt; D: IWFC; U: UKIRT; p02: (Pinfield et al. 2002, in preparation); b96: Basri et al. (1996); h99: Hambly et al. (1999). [1]Moraux et al. (2001); [2]Stauffer et al. (1998); [3]Pinfield et al. (2000); [4]Martín et al. (1998); [5]Hambly et al. (1999); [6]Basri et al. (1996); [7]Festin (1998); [8]Rebolo et al. (1996); [9]Rebolo et al. (1995).

(Moraux et al. 2001). While this may not be a complete surprise given that the candidates from the CFHT survey are included here, it should be borne in mind that this work incorporates mass function points from the independent study of Adams et al. (2001), more than doubles the area sampled by Bouvier et al. (1998) and probes about 2.5 mag deeper over an area comparable in size to the CFHT survey.

The results of detailed N-body simulations that have become available over the last few years (e.g. de la Fuente Marcos & de la Fuente Marcos 2000; Adams et al. 2002) indicate that we can now sensibly compare our result to those obtained recently for young clusters such as σ-Orionis (Bejar et al. 2001) and IC 348 (Najita, Tiede & Carr 2000). For example, fig. 6 of de la Feunte Marcos & de la Feunte Marcos (1999) shows that at an age of 125 Myr

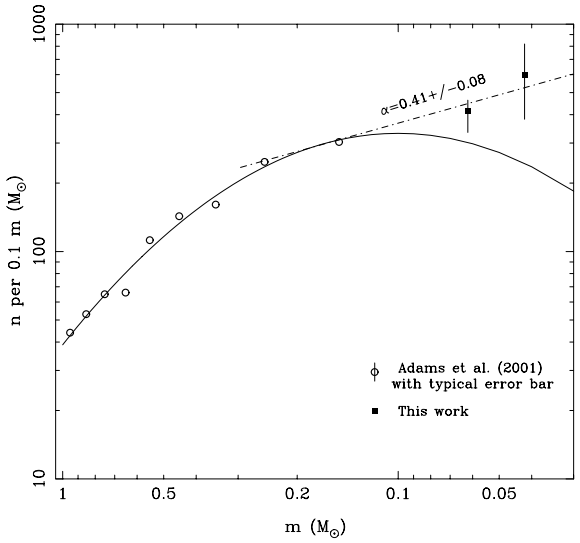

Figure 6. The mass function of the Pleiades cluster from 1–0.04 $M_\odot$ as determined here and by Adams et al. (2001). Overplotted are the best-fit log-normal function to the points of Adams et al. (2001) and the best-fit power law to the four lowest-mass bins.

(∼10 cluster crossing times) despite the total number of cluster members having dropped by ∼10 per cent the fraction of BD members has remained more or less constant. The simulations of Adams et al. (2002), which include a sizeable population of primordial binaries, are entirely consistent with this finding. Bejar et al. (2001) and Najita et al. (2000) report that the mass functions of the 5-Myr-old σ-Orionis and the 3-Myr-old IC348 clusters can be represented by power laws with indices of $\alpha = 0.8 \pm 0.4$ ($0.2\ M_\odot \gtrsim M \gtrsim 0.01\ M_\odot$) and $\alpha = 0.4$ ($0.7\ M_\odot \gtrsim M \gtrsim 0.015\ M_\odot$), respectively. These are consistent with the value determined here for the Pleiades, although the MF of σ-Orionis is only just consistent and could be intrinsically steeper. The mass function of IC 348 and σ-Orionis do not display any evidence for a turn down at the lowest masses. Therefore, by assuming that objects of such low mass were also manufactured in the Pleiades we have extrapolated our power-law mass function model down to the deuterium-burning limit (M = 0.012 $M_\odot$). This extrapolation indicates that the total mass of BDs in the Pleiades is 13^{+4}_{-3} $M_\odot$. Clearly, despite BDs being relatively numerous in the Pleiades, they are not present in sufficient numbers to contribute significantly to the overall mass of the cluster. Pinfield et al. (1998) and Raboud & Mermilliod (1998) found the mass of the cluster to be 735 and 720 $M_\odot$, respectively, and our estimate of the total BD mass in the Pleiades makes up only ∼2 per cent of this.

6 CONCLUSION

We have used new infrared data to reassess the membership status of candidate low-mass Pleiads from the ITP *I Z* survey of Zapatero-Osorio et al. (1999). Those objects with *I–K* colours consistent with cluster membership have been compiled with candidates from three other large optical surveys of the cluster to yield the largest magnitude-limited sample of Pleiades BDs to date. From a detailed analysis of their spatial distribution (using King profiles) we have determined that the core radius of substellar Pleiads is $5.0^{+3.0}_{-1.5}$ pc. This is contrary to the findings of our previous study based on a smaller sample of BDs, which suggested that the core radius had turned over by the substellar regime to a value of $\leqslant$3 pc (Jameson et al. 1999). Instead, this result is consistent with a continuation of the $r_c \propto M^{-0.5}$ trend observed by Pinfield et al. (1998) for higher-mass stellar members, suggesting that the lowest-mass Pleiads are by and large dynamically relaxed. We have used our large sample of substellar cluster members and improved estimate of the BD core radius to place tight constraints on the shape of the mass function across and below the stellar/substellar boundary. We find that a power law with index $\alpha = 0.41 \pm 0.08$ provides an excellent match to the cluster mass function in the regime $0.3\ M_\odot \gtrsim M \gtrsim 0.035\ M_\odot$. This result is not greatly sensitive to our choice of evolutionary model or uncertainties in the cluster age and distance. However, the cluster mass function steepens slightly to $\alpha = 0.50 \pm 0.08$ if we assume a plausible fraction of unresolved binaries (46 per cent).

We have argued that the present-day cluster mass function is a good representation of the IMF and allows for a sensible comparison between our result and those derived for younger clusters. By assuming that the mass function of the Pleiades continues to rise slowly down to the deuterium-burning limit at 0.012 $M_\odot$, we calculate that the mass of all cluster BDs is 13^{+4}_{-3} $M_\odot$. Therefore, while BDs are quite numerous in the Pleiades they only make up ∼2 per cent of its mass. If this result is generally true for the Galactic disc, then BDs do not contribute significantly to the disc dark matter that is inferred from tracer populations (e.g. Bahcall et al. 1992) in approximately equal quantities as the luminous matter.

ACKNOWLEDGMENTS

PDD and DJP acknowledge funding from PPARC. The United Kingdom Infrared Telescope is operated by the Joint Astronomy Centre on behalf of the UK Particle Physics and Astronomy Research Council. This publication makes use of data products from the Two Micron All Sky Survey, which is a joint project of the University of Massachusetts and the Infrared Processing and Analysis Centre/California Institute of Technology, funded by the National Aeronautics and Space Administration and the National Science Foundation. We thank Joseph Adams for making available to us a tabular version of his Pleiades mass function, and finally we thank the referee John Stauffer for useful comments that have improved this work.

REFERENCES

Adams F. C., Fatuzzo M., 1996, ApJ, 464, 256
Adams J. D., Stauffer J. R., Monet D. G., Skrutskie M. F., Beichman C. A., 2001, AJ, 121, 2053
Adams T., Scally A., Davies M. B., Jameson R. F., 2002, MNRAS, 333, 547
Bahcall J. N., Flynn C., Gould A., 1992, ApJ, 389, 234
Baraffe I., Chabrier G., Allard F., Hauschildt P. H., 1998, A&A, 337, 403
Baraffe I., Chabrier G., Allard F., Hauschildt P. H., 2002, A&A, 382, 563
Basri G., Marcy G. W., Graham J. R., 1996, ApJ., 458, 600
Bejar V. J. S. et al., 2001, ApJ, 556, 830
Bessel M. S., 1986, PASP, 98, 1303
Bessell M. S., Castelli F., Plez B., 1998, A&A, 333, 231
Bouvier J., Stauffer J. R., Martín E. L., Barrado y Navascues D., Wallace B., Bejar V. J. S., 1998, A&A, 336, 490
Burrows A., Hubbard W. B., Saumon D., Lunine J., 1993, ApJ, 406, 158
Burrows A. et al., 1997, ApJ, 491, 856
Casali M., Hawarden T., 1992, UKIRT Newsletter, 4, 33
Chabrier G., Baraffe I., Allard F., Hauschildt P., 2000, ApJ, 542, 462
Cossburn M. R., Hodgkin S. T., Jameson R. F., Pinfield D. J., 1997, MNRAS, 287, 180P

Cossburn M. R., Hodgkin S. T., Jameson R. F., Pinfield D. J., 1998, ASP Conf. Ser. 154. Astron. Soc. Pac., San Francisco, p. 1854
Crawford D. L., Perry C. L., 1976, AJ, 81, 419
D'Antona F., Mazzitelli I., 1997, Memorie della Societa Astronomia Italiana, 68, 807
de la Fuente Marcos R., de la Fuente Marcos C., 2000, ApSS, 271, 127
Dobbie P. D., Kenyon F., Jameson R. F., Hodgkin S. T., Pinfield D. J., Osborne S. L., 2002a, MNRAS, 335, 687 (this issue)
Dobbie P. D., Kenyon F., Jameson R. F., Hodgkin S. T., 2002b, MNRAS, 331, 445
Elmegreen B., 2000, MNRAS, 311L, 5
Festin L., 1997, A&A, 322, 455
Festin L., 1998, A&A, 333, 497
Fitzpatrick E., 1999, PASP, 111, 63
Gizis J. E., Monet D. G., Reid I. N., Kirkpatrick J. D., Liebert J., Williams R. J., 2000, AJ, 1 20, 1085
Hambly N. C., Hodgkin S. T., Cossburn M. R., Jameson R. F., 1999, MNRAS, 303, 385
Hawarden T. G., Leggett S. K., Letawsky M. B., Ballantyne D. R., Casali M. M., 2001, MNRAS, 325, 563
Hodgkin S. T., Jameson R. F., Pinfield D. J., Steele I. A., Hambly N. C., 1999, ASP Conf. Ser. 134. Astron. Soc. Pac., San Francisco, p. 99
Jameson R. F., Hodgkin S. T., Cossburn M. R., Pinfield D. J., 1999, ASP Conf. Ser. 134. Astron. Soc. Pac., San Francisco, p. 99
Jameson R. F., Skillen I., 1989, MNRAS, 239, 247
King I. R., 1962, AJ, 67, 471
Kirkpatrick J. D., McGraw J. T., Hess T. R., Liebert J., McCarthy D. W. Jr, 1994, ApJS, 94, 749
Kirkpatrick J. D. et al., 1999, AJ, 519, 802
Landolt A. U., 1992, AJ, 104, 340
Leggett S. K., Allard F., Hauschildt P. H., 1998, ApJ, 509, 836
Luhman K. L., Rieke G. H., Young E. T., Cotera A. S., Chen H., Rieke M. J., Schneider G., Thompson R. I., 2000, ApJ, 540, 1016
Martín E. L., Rebolo R., Zapatero-Osorio M. R., 1996, ApJ, 469, 706
Martín E. L., Basri G., Zapatero-Osorio M. R., Rebolo R., García López R. J., 1998, ApJ, 507, L41
Martín E. L., Delfosse X., Basri G., Goldman B., Forveille T., Zapatero-Osorio M. R., 1999, AJ, 118, 2466
Martín E. L., Brandner W., Bouvier J., Luhman K. L., Stauffer J., Basri G., Zapatero-Osorio M. R., Barrado y Navascuos D., 2000, ApJ, 543, 299
McMahon R. G., Walton N. A., Irwin M. J., Lewis J. R., Bunclark P. S., Jones D. H., 2001, New Astronomy Reviews, 45, 97
Moraux E., Bouvier J., Stauffer J. R., 2001, A&A, 367, 211
Najita J. R., Tiede G. P., Carr J. S., 2000, ApJ, 541, 977
Pinfield D. J., Jameson R. F., Hodgkin S. T., 1998, MNRAS, 299, 955
Pinfield D. J., Hodgkin S. T., Jameson R. F., Cossburn M. R., Hambly N. C., Devereux N., 2000, MNRAS, 313, 347
Pinsonneault M. H., Stauffer J., Soderblom D. R., King J. R., Hanson R. B., 1998, ApJ, 504, 170
Raboud D., Mermilliod J. C., 1998, A&A, 329, 101
Rebolo R., Zapatero-Osorio M. R., Martín E. L., 1995, Nat, 377, 129
Rebolo R., Martín, E. L., Basri G., Marcy W., Zapatero-Osorio M. R., 1996, ApJL, 469, 53
Skrutskie M. F. et al., 1995, AAS, 187, 75.07
Spitzer L., Jr, Mathieu R. D., 1980, ApJ, 241, 618
Stauffer J. R., Hamilton D., Probst R. G., Rieke G., Mateo M., 1989, ApJL, 344, L21
Stauffer J. R., Hamilton D., Probst R. G., 1994, AJ, 108, 155
Stauffer J. R., Schultz G., Kirkpatrick J. D., 1998, ApJ, 499, L199
Steele I. S., Jameson R. F., 1995, MNRAS, 272, 630
van Leeuwen F., 1999, A&A, 341, L71
White R. J., Ghez A. M., Reid I. N., Schultz G., 1999, ApJ, 520, 811
Zapatero-Osorio M. R., Rebolo R., Martín E. L., 1997a, A&A, 317, 164
Zapatero-Osorio M. R., Martín E. L., Rebolo R., 1997b, A&A, 323, 105
Zapatero-Osorio M. R., Martín E. L., Rebolo R., Basri G., Magazzu A., Hodgkin S. T., Jameson R. F., Cossburn M. R., 1997c, ApJL, 491, 81
Zapatero-Osorio M. R., Rebolo R., Martín E. L., Hodgkin S. T., Cossburn M. R., Magazzu A., Steele I. A., Jameson R. F., 1999, A&A, Supp., 134, 537

This paper has been typeset from a TEX/LATEX file prepared by the author.